Application of Cosserat Continuum Approach in the Finite Element Shear Strength Reduction Analysis of Jointed Rock Slopes

Riahi, Azadeh
Lassonde Institute, Department of Civil Engineering, University of Toronto, Toronto, Canada

Curran, John H.
Lassonde Institute, Department of Civil Engineering, University of Toronto, Toronto, Canada
Rocscience Inc., Toronto, Canada

Keyword: Cosserat theory, Equivalent Continuum, Shear Strength Reduction

ABSTRACT: This paper focuses on the application of a continuum-based method in the Shear Strength Reduction (SSR) analysis of the stability of jointed rock slopes. In order to take into account the jointed nature of the material, the Finite Element Method (FEM) is formulated based on Cosserat theory. Also, it is assumed that failure of the equivalent material can result from failure of the joints, failure of intact material, or a combinatory mechanism. A consistent elasto-plastic algorithm which takes into account the failure of multiple plastic surfaces at the FEM integration points is adopted. The deformation mode, failure mechanism, and factor of safety predicted by the proposed model are verified against two discontinuous models, including the Discrete Element Method (DEM) and the FEM explicit interface model. The results indicate that the Cosserat continuum approach is a reliable tool for identifying various modes of failure of jointed slope problems. In addition, application of a robust and accurate elasto-plastic algorithm based on the multi-surface plasticity concept enables the method to predict the factor of safety accurately.

1 Introduction

In computational geomechanics, two main approaches have been adopted to simulate jointed materials: 1) techniques which explicitly take into account the discontinuous nature of joints, i.e., Discontinuous Displacement Analysis (DDA), Discrete Element Method (DEM), and Finite Element Method (FEM) or Finite Difference Method (FDM), which utilizes an interface element, and 2) smeared techniques based on an equivalent continuum concept, i.e., an FEM or FDM equivalent continuum based on classical anisotropic models.

SSR (Dawson et al., 1999; Griffiths and Lane, 1999; Hammah et al., 2005) has proven to be an efficient tool in the analysis of slope stability problems for materials exhibiting both a discrete and a continuous nature. However, due to the discrete nature of jointed rocks, often it is combined with DDA or DEM analysis of rock slopes with a layered or blocky structure. Recently, Hammah et al. (2007) demonstrated that the SSR-FEM which utilizes an explicit interface element can be a reliable technique in the stability analysis of this class of geostructures. In discontinuous methodology, joints are explicitly simulated, which makes the definition of the geometry of the input model a tedious task, especially as the number of joints increases. Consequently, the equivalent continuum approach or ubiquitous joint model has grown in popularity, where the original discontinuous material is replaced by an anisotropic continuous material. However, the ubiquitous joint model based on the classical continuum theory is known to be inapplicable when the internal length scale of the problem (block size or layer thickness) is not negligible compared to dimensions of the engineering problem. Micropolar or Cosserat theory, on the other hand, provides an accurate description of the mechanics of materials with an internal length scale. Cosserat theory was first proposed by the Cosserat brothers at the beginning of the past century (Cosserat, 1909). Later, prominent researchers such as Mindlin (1965) and Kroner (1967) were attracted to its theoretical aspects. Micropolar theory is based on the assumption that micromoments exist at each point of the continuum. A direct consequence of the application of Cosserat theory is that the internal length scale of the material is introduced into the constitutive equations of the system. Subsequently, it provides an enhanced continuum description of the mechanics of discrete materials, such as jointed rock, whose behaviour is governed by an internal length scale (e.g. joint spacing). Application of micropolar theory to the FEM analysis of layered and blocky materials was proposed by Mühlhaus, (1993) and subsequently, was continued by Adhikary and Dyskin, (1997, 1998)

In this paper, the SSR method is applied to a number of slope stability problems simulated by the FEM

Cosserat approach. In contrast to most of the previous works that only allow for the plastic deformation of the interface, in this research, plastic failure within the intact material is also considered. A full three-dimensional (3D) elasto-plastic formulation of Cosserat theory is implemented in the KGC finite element code (University of Toronto). Three examples which involve different mechanisms of failure were investigated using the developed method. In each case, the FEM Cosserat results are compared to the results predicted by the DEM using the UDEC numerical package (Itasca Consulting Group, Inc., 2004), reported by Duncan and Mah, (2004), and the FEM explicit joint model using Phase^2 (Rocscience Inc., 2005), reported by Hammah et al., (2007). Comparison of different aspects of the results verifies that by introducing the internal length scale or bending stiffness of layers into the constitutive equations, the FEM continuum-based approach becomes capable of capturing modes of failure such as flexural layer bending that could be identified only by discontinuous models. Also, application of a multi-surface plasticity algorithm is an essential aspect in a continuum-based analysis of jointed slope problems that often involve more than one failure mechanism.

2 Introduction to Cosserat theory

Cosserat theory is based on the assumption that micromoments exist at each point of a continuum. The governing equations of the Cosserat continuum can be expressed by:

$$\sigma_{ij,i} + b_j = 0 \tag{1}$$

$$m_k + \mu_{kj,j} - e_{kij}\sigma_{ij} = 0 \tag{2}$$

where b is the body force, m is the body couple moment and σ and μ are Cosserat stress and Cosserat couple stress or moment stress, respectively. In Cosserat theory, the stress tensor is generally not symmetric, and the difference in the shear components of stress is equilibrated by micromoments. Compared to the classical continuum, the enhanced or Cosserat continuum is obtained by adding an independent rotation, to each point of the continuum, which is different from the rotation of the material points. The Cosserat rotation is defined as the independent rotation of a rigid triad attached to each material point which rotates independently with respect to the material triad. Thus, in 3D analysis, each node is associated with 3 displacement and 3 rotational degrees of freedom. The vector of nodal degrees of freedom is defined by:

$$\left[\mathbf{u},\boldsymbol{\theta}\right] = [u_1 \quad u_2 \quad u_3 \quad \theta_1^c \quad \theta_2^c \quad \theta_3^c] \tag{3}$$

In layered materials, the Cosserat rotation allows for slip or discontinuity in deformation at the interface of layers. The Cosserat strain measure, γ , then can be expressed by:

$$\gamma_{ij} = u_{j,i} - e_{ijk}\theta_k^c \tag{4}$$

where e_{ijk} is the permutation symbol. Also, a second measure of strain or curvature, κ , is introduced into the formulation. Curvature represents the variation of rotations of the adjacent triads, and is expressed by:

$$\kappa_{ij} = \theta^c_{i,j} \tag{5}$$

2.1 The elasticity matrix of a layered Cosserat material

For the derivation of the components of the elasticity tensor, the equivalent continuum concept is considered. It is assumed that a jointed material consists of an intact matrix and a number of discontinuous surfaces which are called interfaces or joints. From a mathematical point of view, such a material can be simplified to a number of elasto-visoplastic modules interacting in series (Sharma and Pande, 1988). The elasticity matrix of the equivalent continuum can be calculated based on the elastic properties of the different components of a material using the following equations:

$$D_{Eq} = D_{matrix} + D_{j1} + .. + D_{jn} \text{ , and } \frac{1}{C_{Eq}} = \frac{1}{C_{matrix}} + \frac{1}{C_{j1}} + ... + \frac{1}{C_{jn}} \tag{6}$$

where D denotes the compliance and C denotes the elasticity tensor, and sub-indices Eq and *j* denote equivalent continuum and joints, respectively.

In Cosserat continuum theory, the elasticity tensor is a block diagonal matrix that relates the stress tensor $\hat{\sigma}$, and couple stress tensor, $\hat{\mu}$, to their work conjugate measures, $\hat{\gamma}$, and , $\hat{\kappa}$, through:

$$\begin{pmatrix} \hat{\sigma} \\ \hat{\mu} \end{pmatrix} = D\begin{pmatrix} \hat{\gamma} \\ \hat{\kappa} \end{pmatrix} = diag(D_1, D_2)\begin{pmatrix} \hat{\gamma} \\ \hat{\kappa} \end{pmatrix} \tag{7}$$

where the $\wedge$ sign denotes the local coordinates of anisotropy i.e., local coordinates of the joints. The difference between Cosserat theory and classical continuum theory is in the way that shear stresses are distributed, and the way that micromoments are related to their work conjugate curvature measures. Considering the 2D representation of a beam depicted in Figure 1, it can be interpreted that part of each shear stress component along the thickness of the layer , i.e., σ_{13} is in equilibrium with its conjugate shear component σ_{31} and is related to the corresponding strain components through the shear coefficient of the equivalent continuum, G_{11}, expressed by:

$$\sigma_{31} = G_{11}(\gamma_{13} + \gamma_{31})\,;\; G_{11} = 1/\left(\frac{1}{G} + \frac{1}{hk_s}\right) = \frac{Ghk_s}{G + hk_s} \tag{8}$$

where G is the shear modulus of the intact material, h is the layer thickness and k_s is the shear stiffness of the joints. However, the stress occurring on a plane perpendicular to the axis of the beam has a contribution from the bending of the layers, which is related to γ_{13} through the shear modulus of the individual layers, G. Thus the stress component perpendicular to the layers can be expressed as:

$$\sigma_{13} = G_{11}(\gamma_{13} + \gamma_{31}) + G\gamma_{13} \tag{9}$$

Also, the nonzero couple stress, μ_{31}, can be related to the curvature of the system through the bending stiffness of the interacting layers, as follows:

$$\mu_{31} = B\kappa_{31}\,;\; B = \frac{Eh^2}{12(1-\upsilon^2)}\left(\frac{G - G_{11}}{G + G_{11}}\right) \tag{10}$$

where E and υ are the Young's modulus and Poisson's ratio of the layers. It is clear that Equation 10 accounts for the effect of internal length scale or layer thickness. For a comprehensive study on the mechanical considerations in the derivation of Cosserat parameters, and the 2D elasticity matrix of a Cosserat layered material one can refer to (Zvolinski & Shkhinek, 1984) and (Mühlhaus, 1995), respectively.

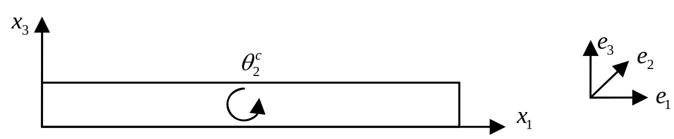

Figure 1 2D representation of a single beam.

2.2 Elasto-plastic behaviour of the equivalent continuum

In this research, it is assumed that failure of the equivalent continuum can be due to the failure of each set of joints or failure of the intact material, which are simultaneously present at all FEM integration points. Each component exhibits a separately specified strength and post-peak behaviour. Once the stress level at a point reaches the strength of any of these components, its corresponding mechanism becomes active, and its potential rule is mobilized. For the intact rock two yield criteria expressing shear and tensile failure were considered. Shear failure of the intact rock is expressed by an isotropic Mohr-Coulomb law:

$$F_1 = |\tau| + \sigma_n \tan\varphi - c = 0 \tag{11}$$

where φ is the friction coefficient and c is the cohesion parameter. Mohr-Coulomb criterion for isotropic materials can be written in the following form in stress invariants space:

$$F_1 = \frac{I_1}{3}\sin(\varphi) + \sqrt{J_2}\left[\cos(\varphi) - \frac{1}{\sqrt{3}}\sin(\theta^L)\sin(\varphi)\right] - c\cos(\varphi) \tag{12}$$

where I is the first invariant of the stress tensor, J_2 is the second invariant of deviatoric part of the stress, and θ^L is the Lodé angle. Also, the tensile strength of the intact rock is expressed by:

$$F_2 = \sigma_1 - c_t = \frac{2}{\sqrt{3}}\sqrt{J_2}\sin(\theta^L + \frac{2\pi}{3}) + \frac{I_1}{3} - c_t = 0 \tag{13}$$

where σ_1 is the maximum principal stress, and c_t is the tensile strength of the material. Strength of the joints also follows a Mohr-Coulomb type behaviour combined with a tensile failure surface. In order to take into account the orientation dependence properties of the anisotropic material, the stress tensor is projected onto the surface of the joints. The violation of yield functions is checked in the local coordinate of the joints as follows:

$$F_1 = \left| \sqrt{\hat{\sigma}_{31}^2 + \hat{\sigma}_{32}^2} \right| + \hat{\sigma}_{33} \tan \varphi - c = 0 \tag{14}$$

and

$$F_2 = \hat{\sigma}_{33} = 0 \tag{15}$$

where $\hat{x}_3$ is the normal vector to the interface and $\hat{\sigma}$ is the stress expressed in the local coordinates of the joint as:

$$\sigma = Q \hat{\sigma} Q^T \tag{16}$$

where Q is the orthogonal transformation matrix for change of coordinate system of a second order tensor.

In the post-peak analysis, it is assumed that the shear failure of the intact rock and joints follows a non-associative flow rule with a dilatancy angle of φ_{dil}, while the tensile failure of both components always follows an associative rule.

Finally, in Cosserat plasticity theory, the effect of micromoments should be taken into consideration. It is clear that both the yield and potential functions of the interface depend only on the normal and shear components of stress occurring on the surface (Adhikary and Dyskin, 1998; Dawson and Cundall, 1992). Yielding within the intact rock on the other hand, depends on the values of the micromoments of the system and consequently involves a more complicated mechanism. The effect of micromoments on the strength of the intact material can be described based on beam theory (Adhikary and Guo, 2002). However, the significance and the effect of micromoments in both shear and tensile failure of layers requires extensive analytical and experimental research. In the present work, the plasticity formulation of the intact material is based on the symmetric part of the stress tensor, and effects of micromoments are disregarded. Clearly, the approach provides an estimate to the exact solution. Nevertheless, results show a high level of consistency with other numerical methods.

2.3 Stress integration of multiple plastic surfaces

The essence of the elasto-plastic relation in the presence of multiple mechanisms is similar to the case of a single yield surface, i.e.:

$$\dot{\varepsilon}_{ij} = \dot{\varepsilon}_{ij}^e + \dot{\varepsilon}_{ij}^p \tag{17}$$

and

$$\dot{\sigma}_{ij} = D_{ijkl} \dot{\varepsilon}_{ij}^e \tag{18}$$

In materials with multiple mechanisms, the total increment of plastic strain is obtained by the summation of the plastic straining of all active plasticity surfaces. This can be expressed by:

$$\dot{\varepsilon}_{ij}^p = \sum_{\alpha=1}^{n} \left(\dot{\varepsilon}_{ij}^p \right)_\alpha = \sum_\alpha \dot{\lambda}_\alpha \frac{\partial Q_\alpha}{\partial \sigma_{ij}} \tag{19}$$

where α denotes the index of activated surfaces and Q_α is the corresponding potential surface. From a numerical point of view, the existence of multiple yield mechanisms can result in serious complications in the determination of the activated surfaces and the post-peak behaviour. The FEM integration algorithm adopted in this research belongs to the multi-surface plasticity schemes discussed by Simo (1988) and Pasternack and Timmerman (1986) It should be noted that in the presence of multiple failure mechanisms, violation of the yield criterion does not guarantee that the corresponding mechanism is active, i.e., positiveness of plastic multipliers, $\dot{\lambda}_\alpha$, indicate the active plastic surfaces.

3 Overview of the Shear Strength Reduction Method

The SSR has proven to be an efficient tool in the analysis of slope stability problems for materials exhibiting both a discrete and a continuous nature. In this method a systematic search is performed to find the reduction factor, F_s, that brings the slope to the limit of failure. The reduced shear strength of a Mohr-

Coulomb material is described by the following equation, in which $c^* = c/F_s$ and $\varphi = \arctan(\tan(\varphi^*)/F_s)$ are factored Mohr-Coulomb shear strength parameters.:

$$\frac{\tau}{F_s} = \frac{c}{F_s} + \sigma_n \frac{\tan(\varphi)}{F_s}, \text{ or } \frac{\tau}{F_s} = c^* + \sigma_n \tan(\varphi^*) \tag{20}$$

The factor of safety is the maximum value of F_S for which the numerical solution remains stable. The problem should be solved for different values of F_S. A sudden increase in values of displacements in the graph of F_S versus maximum displacement indicates the onset of instability. Also, non-convergence of the solution within a reasonably specified tolerance and number of iterations is an indicator of failure in the FEM solution (Hammah et al., 2007).

4 Examples

Three different examples were chosen to demonstrate the performance of the proposed FEM Cosserat continuum approach to the slope stability analysis of layered rock slopes using the SSR method. The geometry of the slope and the FEM mesh of the Cosserat model are depicted in Figure 2.
For the intact rock, an isotropic material with Young's modulus of $9.072\,GPa$ and a Poisson's ratio of 0.26 was considered. The joints have a normal stiffness, k_n, and a shear stiffness, k_s, of $100\,MPa/m$ and $10\,MPa/m$, respectively. For the elasto-plastic behaviour of the intact rock, a non-associative Mohr-Coulomb failure criterion with a friction coefficient of 43°, dilation angle of 0°, and cohesion of $675\,KPa$, with zero tensile strength, was considered. In examples 4.1 and 4.3, the joints exhibit a Mohr-Coulomb failure criterion with a friction coefficient of 40°, dilation angle of 0°, cohesion parameter of $100KPa$, and tensile strength of $100KPa$. In example 4.2 the cohesion and tensile strength of the joints were set to 0. The load was applied incrementally in a total number of 30 steps and the tolerance of the solution was set to 0.001. The results were verified against the results predicted by DEM using UDEC numerical package (Duncan and Mah, 2004), and the FEM explicit joint model using Phase[2] (Hammah et al., 2007).

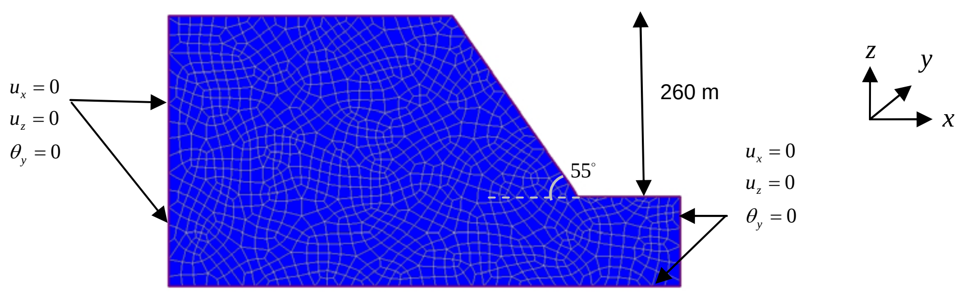

Figure 2 Slope geometry, boundary conditions, and the FEM mesh for Cosserat solution of slope stability examples**.**

4.1 Slope with daylighting joints

The joints in this example are approximately $21\,m$ apart and dipping at 55°. The factor of safety predicted by the FEM Cosserat solution was 1.27 (see Figure 3b), while UDEC predicted 1.28, and the FEM explicit joint model predicted 1.32. The failure mechanism predicted by the Cosserat solution is depicted in Figure 3a. Similar to the failure mechanism identified by UDEC and Phase[2] (see Figure 4), the FEM Cosserat solution indicates that the mechanism of failure is a combination of sliding at the toe and a curved tension crack at the top of the slope. The failure mechanism for the FEM Cosserat solution was determined based on the contours of the total displacements and the deformed shape of the slope, and contours of the effective plastic straining of the activated plastic surfaces. Since progressive slip on the joint plane is the dominant mode of failure, the bending rigidity of the layers does not have a significant effect on the stability of this slope.

4.2 Plane Failure of slope with non-daylighting joints

The joints in this example are spaced at approximately $20\,m$ and dipping at 70°. The factor of safety predicted by the FEM Cosserat solution is 1.45 (see Figure 5b), while UDEC predicted 1.5, and the FEM explicit joint model predicted 1.53. The failure mechanism predicted by the Cosserat model (see Figure 5a) is a combination of shearing through the intact rock in the lower part, near the toe of the slope, and sliding along joints in the upper part of the slope. The failure mechanism predicted by UDEC and the FEM explicit joint model is depicted in Figure 6. In this example, the bending rigidity of the inclined columns of rock sustains part of the applied load.

4.3 Failure involving flexural toppling

The slope in this example has a single set of joints, approximately $20\ m$ apart, which dip 70° into the slope face. The FEM Cosserat model predicts a safety factor of 1.45 (see Figure 7b), while UDEC analysis gives 1.3, and the FEM explicit joint model predicts 1.41. Similar to the FEM explicit joint model and UDEC analysis, the FEM Cosserat joint model identifies the mode of failure to be flexural bending of the rock columns (see Figures 7a and 8). However, it yields a relatively high SSR factor compared to the other models, which is due to underestimating the tensile forces within the intact rock. The tensile cracking is due to the bending of layers or high values of curvatures. It can be explained using beam theory that the presence of bending moments in a beam will result in axial stress along the layers. By neglecting the effect of the bending stiffness of the layers, the Cosserat model reduces to the classical ubiquitous joint model. Since in this example, the bending rigidity of the layers sustains the applied load, the classical model totally fails in predicting the mode of deformation of the layers, and consequently cannot capture the correct mechanism of failure.

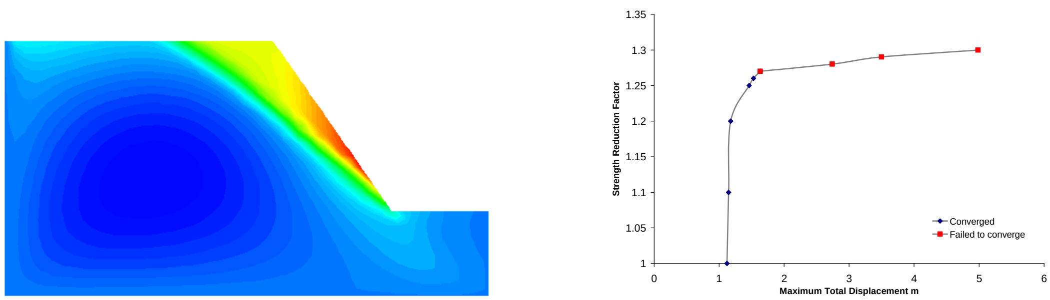

(a) (b)

Figure 3 a) Failure mechanism based on contours of total displacement and b) displacement versus SSR factor predicted by the FEM Cosserat solution for a slope with daylighting joints.

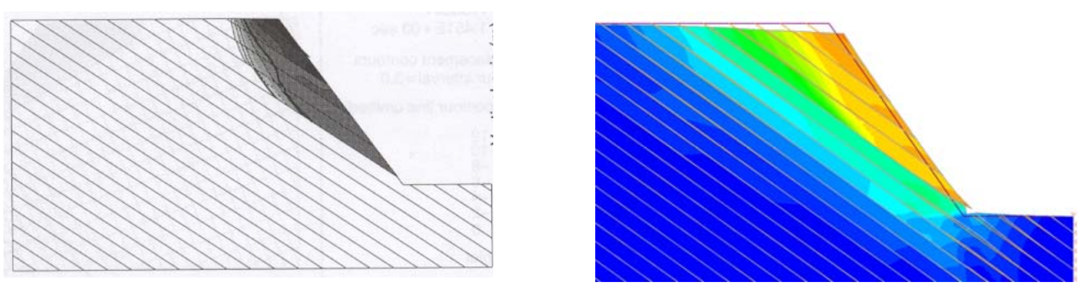

(a) (b)

Figure 4 Failure mechanism and contours of total displacement for a slope with daylighting joints predicted by: a) UDEC and b) Phase^2 FE-SSR.

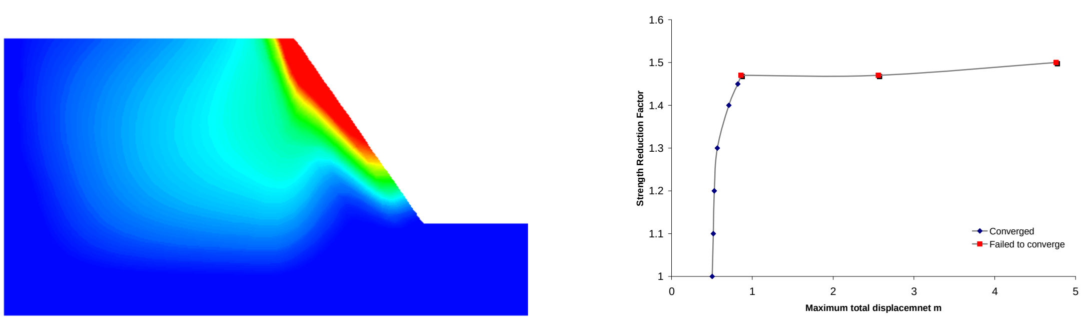

(a) (b)

Figure 5 a) Failure mechanism based on contours of total displacement and b) displacement versus SSR factor predicted by the FEM Cosserat solution for a slope with non-daylighting joints.

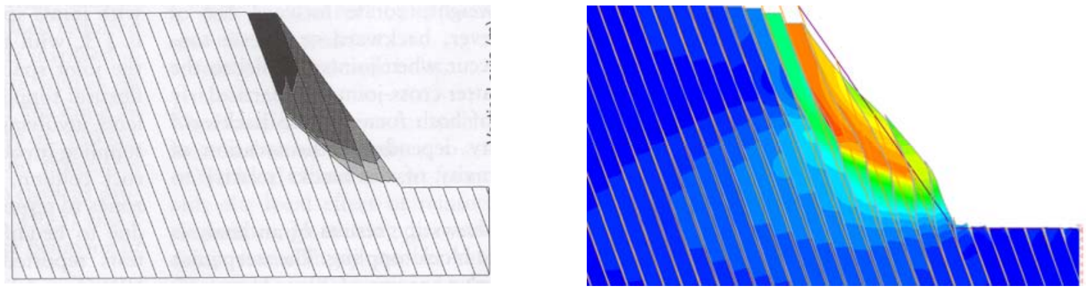

(a) (b)

Figure 6 Failure mechanism and contours of total displacement for a slope with non-daylighting joints predicted by: a) UDEC and b) Phase[2] FE-SSR.

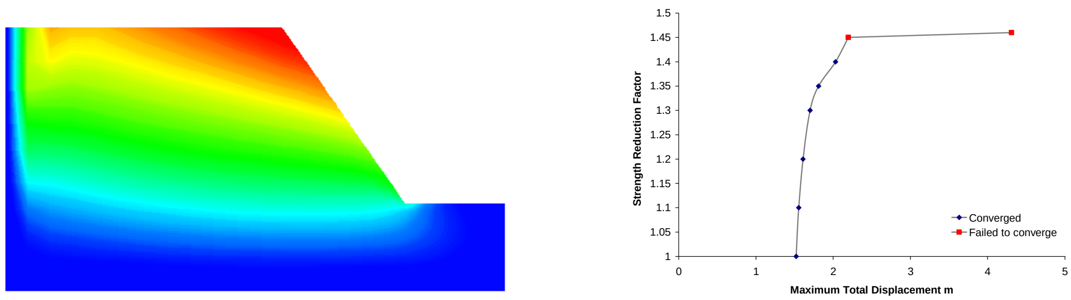

(a) (b)

Figure 7 a) Failure mechanism based on contours of total displacement and b) displacement versus SSR factor predicted by the FEM Cosserat solution for a slope exhibiting flexural bending.

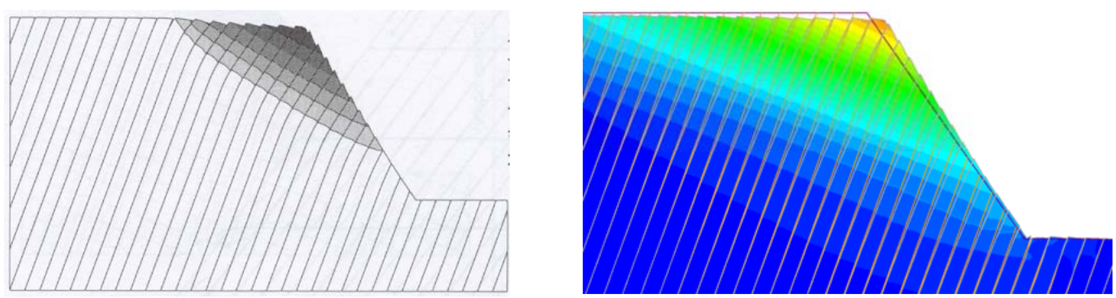

(a) (b)

Figure 8 Failure mechanism and contours of total displacement for a slope exhibiting flexural bending predicted by: a) UDEC and b) Phase[2] FE-SSR.

5 Conclusion

The main focus of this paper was to investigate the performance of the FEM continuum-based technique in the stability analysis of discrete or jointed materials. The results predicted by the proposed FEM Cosserat model were verified against two different discontinuous methods. The comparison was based on the deformation mode, failure mechanism, and values of the SSR factor.

Classical continuum theory is based on the assumption of the continuity of deformation, and, as a result, if the internal length scale is comparable to dimensions of the problem, the FEM solution formulated in classical continuum theory can introduce large errors into the solution. Alternatively, Cosserat theory provides an enhanced continuum description of materials with microstructures. In the FEM Cosserat solution, the bending stiffness of layers is introduced into the governing equations of the system; subsequently, the method becomes capable of capturing modes of failure such as flexural layer bending that can be identified only by discontinuous models. Experimental observation of the failure of jointed rock slopes clearly indicates that the ultimate collapse often involves the failure of different components of the material. Numerical prediction of the failure mechanism depends on capturing the deformation mode and the correct formulation of the strength and post-peak behaviour of the material. The Cosserat continuum approach was further improved by applying a multi-surface plasticity algorithm which allows for simultaneous failure of different components of the material. In total, four plastic surfaces could be potentially active at each point of the continuum. Consistency between values of the SSR factor obtained by this method and values predicted by discontinuous models clearly indicate the accuracy of the integration algorithm in the presence of multiple plastic surfaces.

It was found that the mode of failure and deformation is greatly influenced by the effect of bending stiffness or layer thickness. It should be noted that in addition to physical parameters, values of the SSR factor predicted by the FEM can be affected by a number of numerical aspects such as the stability and accuracy of the stress update integration scheme as well as the FEM mesh size.

The results clearly suggest that the FEM Cosserat model can be an efficient and reliable tool in the stability analysis of jointed rock slope problems. An attractive aspect of the FEM Cosserat solution is the fact that discontinuity surfaces are not explicitly modeled, and that the solution can be performed by an FEM discretization which is totally independent of joint spacing and orientation. In conclusion, the FEM Cosserat solution can be an important tool in slope stability analysis of 3D problems with arbitrarily-orientated layers.

6 References

Adhikary, D. P., Dyskin, A. V. (1997). A Cosserat continuum for layered materials, Computers and Geomechanics, 20(1), 15-45.

Adhikary, D. P., Dyskin, A. V. (1998). A continuum model of layered rock masses with non-associative joint plasticity, International Journal for Numerical and Analytical Methods in Geomechanics, 22(4), 245-261.

Adhikary, D. P., Guo, H. (2002). An orthotropic Cosserat elasto-plastic model for layered rocks, Rock Mechanics and Rock Engineering, 35(3), 161-170.

Cosserat, E. (1909). In Cosserat F. (Ed.), Theorie des corps deformables, Paris, Hermann.

Dawson, E M, Cundall P A (1993). Cosserat plasticity for modeling layered rock, Proceeding the conference on fractured and jointed rock masses, Lake Tahoe, International Journal of Rock Mechanics and Mining Sciences & Geomechanics Abstracts, 30(4), A238.

Dawson, E. M., Roth, W. H., Drescher, A. (1999). Slope stability analysis by strength reduction, Geotechnique, 49(6), 835-840.

Duncan C. W., Mah C.W (2004), Rock slope engineering, Chapter 10, 218-244, Spon Press

Griffiths, D. V., Lane, P. A. (1999). Slope stability analysis by finite elements, Geotechnique, 49(3), 387-403.

Hammah, R. E., Yacoub, T., Corkum, B., Wibowo, F., Curran, J. H. (2007). Analysis of blocky rock slopes with finite element shear strength reduction analysis, Proceeding the 1st Canadian-US rock mechanics symposium, Vancouver, Canada.

Hammah, R. E., Yacoub, T. E., Corkum, B., Curran, J. H. (2005). A comparison of finite element slope stability analysis with conventional limit-equilibrium investigation, Saskatoon, Canada.

Itasca Consulting Group, Inc. (2004). UDEC - Universal Distinct Element Code.

Kroner, E. (1967). Mechanics of generalized continua. In E. Kroner (Ed.), Proceeding IUTAM symposium. generalized Cosserat continuum and continuous theory of dislocations with applications, Berlin, Springer-Verlag.

Mindlin, R. D. (1965). Second gradient of strain and surface-tension in linear elasticity, International Journal of Solids and Structures, 1(4), 417-438.

Mühlhaus, H. B. (1993). Continuum models for layered and blocky materials, Comprehensive rock mechanics, 209-230, Pergamon Press.

Mühlhaus, H. B. (1995). Continuum models for materials with microstructure, Chichester; Toronto, Wiley.

Pasternack, S. Timmerman, D. (1986). On the numerical implementation of an elasto-plastic two surface material model. Computers and Geomechanics, 2(5), 275-307.

Rocscience Inc. (2005). Phase2 v6.0 – two-dimensional finite element slope stability analysis.

Sharma, K. G.,,(1988). Stability of rock masses reinforced by passive, fully-grouted rock bolts. Oxford, Pergamon Press.

Simo, J. C., (1988). Non-smooth multi-surface plasticity and viscoplasticity. Loading/unloading conditions and numerical algorithms. International Journal for Numerical Methods in Engineering, 26(10), 2161

Zvolinski, N. V, Shkhinek, K. N. (1984). Continuum model for a laminar elastic medium. Solid Mechanics, 19(1), 1-9

The paper may be considered for
(Please indicate your choice by putting √ in the appropriate box)

1. Oral Presentation	*
2. Poster Session	